Conformational Complexity in Seven-Membered Cyclic Triazepinone/Open Hydrazones. 2. Molecular Modeling and X-ray Study

Mario F. Simeonov,[†] Ferenc Fülöp,[‡] Reijo Sillanpää, and Kalevi Pihlaja*

Department of Chemistry, University of Turku, FIN-20014 Turku, Finland

Received December 11, 1996[⊗]

The thermodynamic parameters obtained from NMR experiments are compared with the results of theoretical (molecular mechanics MMX and semiempirical AM1, PM3, and MNDO MO) calculations and of X-ray measurements to acquire an additional insight into the dynamic processes of these seven-membered benzoheterocycles.

Introduction

Attempts at clarification have been made both experimentally (mainly NMR spectroscopy) and theoretically (mainly molecular mechanics calculations) for the most stable conformations and the interconversion mechanisms of cycloheptenes,[1] benzocycloheptenes,[1a,2] seven-membered benzoheterocycles, and other related heterocyclic compounds.[3] Most of these studies suggest that the chair form (**C**) has the lowest energy for both cycloheptenes and benzocycloheptenes, although some disagreement appears to exist as to the nature of the transition state conformation for the most likely interconversion pathway. Thus, Allinger and Sprague[16] predicted a conformer with six coplanar carbon atoms for cycloheptene, whereas Kabuss *et al.*[1c] proposed five coplanar carbon atoms. Simple carbocyclic derivatives of cycloheptene have very low $\Delta G^{\ddagger}$ values,[1a] and replacement of the ring carbons by heteroatoms causes such constraints that the barriers to interconversion become higher.[3a]

Recently, through the combined use of NMR, X-ray, and molecular modeling, the structural and energetic aspects of the ring inversion of some 1,4-benzodiazepin-2-ones,[4a] imidazo-1,4-benzodiazepine,[4b] and the benzodiazepine receptor model KC-2846[4c] were also studied. A nonplanar (on the NMR time scale) rapidly interconverting boat-shape conformation was established for the diazepine ring in these 1,4-benzodiazepines and related 2,4-benzodiazepines[4d] and benzotetrazolotriazepines[4e] resembling that found in several X-ray analyses. Special attention was paid to the boat (**B**) and different half-chair (**HC**) conformations, and the semiempirical PM3 level was applied to some of these therapeutically highly active compounds.[5a] For sterically congested derivatives, **B** proved to be the most stable conformation, but the **HC** form was found the most stable for 1,3-cycloheptadiene, 2,3-dihydro-1,4-1*H*-diazepine, and 2,3-dihydro-1*H*-1,4-benzodiazepine.[5a] The relative energies of some tetrahydroazepines and benzazepines have also been calculated with molecular mechanics, AM1 semiempirical, and ab initio methods.[5b]

The idea that biological activity of the benzotriazepines (mainly as psychotherapeutic agents)[5] depends not only on the pharmacophoric grouping[4c] but also on the conformation of the seven-membered ring in the biological fluids[3c] makes the present potentially active and structurally related compounds attractive for a computational study. To our knowledge, no experimental and/or computational study on compounds related to our 1,3,4-benzotriazepin-5-ones exists, with the exception of the *cis*−*trans* isomerization at the annelation of the hetero ring of some 1,3,4-benzotriazepinones.[3b]

The above findings impelled us to set two goals for this initial work: (i) by means of 1D and 2D NMR studies at variable temperature, to characterize the complex conformational properties of compounds **1**−**22** (Scheme 1, Part 1[6a]) in different solvents and (ii) to compare the calculated MMX energies (ΔE) and heats of formation

Scheme 1. Compounds under Study

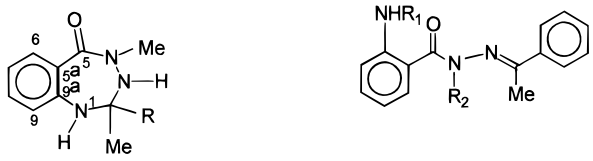

1 R = Me
2 R = *i*-Pr
3 R = *t*-Bt
4 R = Ph

5 R_1 = H R_2 = H
6 R_1 = Me R_2 = Me

[†] Institute of Organic Chemistry with Center of Phytochemistry, Bulgarian Academy of Sciences, BG-1113 Sofia, Bulgaria.

[‡] Institute of Pharmaceutical Chemistry, Albert Szent-Györgyi Medical University, H-6720 Szeged, POB 121, Hungary.

[⊗] Abstract published in *Advance ACS Abstracts,* July 1, 1997.

(1) (a) St-Jacques, M.; Vaziri, C. *Can. J. Chem.* **1973**, *51*, 1192. (b) Allinger, N. L.; Sprague, J. T. *J. Am. Chem. Soc.* **1972**, *94*, 5734. (c) Kabuss, S.; Schmid, H. G.; Friebolin, H.; Faisst, W. *Org. Magn. Reson.* **1970**, *2*, 19. (d) Hendrickson, J. B. *J. Am. Chem. Soc.* **1961**, *83*, 4537. (e) Ermer, O.; Lifson, S. *J. Am. Chem. Soc.* **1973**, *95*, 4121. (f) Zuccarello, F.; Buemi, G.; Favini, G. *J. Mol. Struct.* **1973**, *18*, 295.

(2) Kabuss, S.; Lüttringhaus, A.; Friebolin, H.; Schmid, H. G.; Merke, R. *Tetrahedron Lett.* **1966**, 719.

(3) (a) Wasylishen, R. E.; Rice, K. C.; Weiss, U. *Can. J. Chem.* **1975**, *53*, 414. (b) Gál, M.; Pallagi, I.; Sohár, P.; Fülöp, F.; Kálmán, A. *Tetrahedron* **1989**, *45*, 3513. (c) Aversa, M. C.; Giannetto, P.; Romeo, G.; Ficarra, P.; Vigorita, M. G. *Org. Magn. Reson.* **1981**, *15*, 394. (d) Malik, F.; Hassan, M.; Rosenbaum, D.; Duddeck, H. *Magn. Reson. Chem.* **1989**, *27*, 391.

(4) (a) Gilman, N. W.; Rosen, P.; Earley, J. V.; Cooke, C. M.; Todaro, L. J. *J. Am. Chem. Soc.* **1990**, *112*, 3969. (b) Gilman, N. W.; Rosen, P.; Earley, J. V.; Cook, C. M.; Blount, J. F.; Todaro, L. J. *J. Org. Chem.* **1993**, *58*, 3285. (c) Finner, E.; Zeugner, H.; Benson, W. *Arch. Pharm. (Weinheim)* **1989**, *322*, 507. (d) Sanner, M. A.; Josef, K.; Johnson, R. E.; Dambra, Th.; Kowalczyk, P.; Kullnig, R. K.; Michaels, F. *J. Org. Chem.* **1993**, *58*, 6417. (e) Katritzky, A. R.; Fan, W.-Q.; Greenhill, J. V.; Steel, P. J. *J. Org. Chem.* **1991**, *56*, 1299.

(5) (a) Messinger, J.; Buss, V. *J. Org. Chem.* **1992**, *57*, 3320. (b) Alkorta, I.; Villar, H. O.; Cachau, R. E.; *J. Comput. Chem.* **1993**, *14*, 571. (c) Borea, P. A.; Dean, P. M.; Martin, I. L.; Perkins, T. D. *Mol. Neuropharmacol.* **1992**, *2*, 261. (d) De Sarro, G. B.; Zappala, M.; Grasso, S.; Chimirri, A.; Spagnolo, C.; De Sarro, A. *Mol. Neuropharmacol.* **1992**, *1*, 195.

S0022-3263(96)02323-7 CCC: $14.00

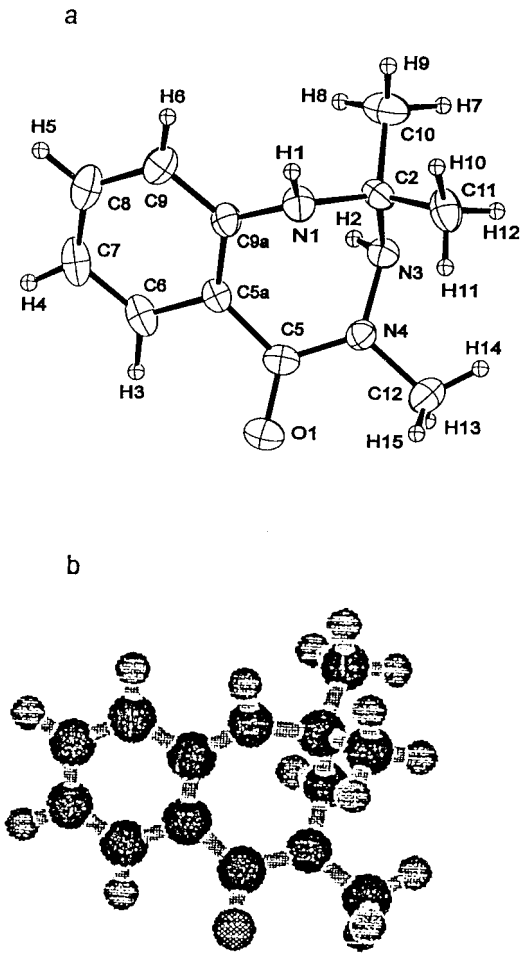

Figure 1. Molecular structure of **1**: (a) structure in the crystal (ORTEP drawing) and (b) PM3-calculated boat (**B**) conformation.

($\Delta H_f°$) of different possible conformers obtained by a variety of computational methods [molecular mechanics (MM),[6b] and semiempirical MNDO,[7] AM1,[8] and PM3[9]] with the experimentally obtained structural and thermodynamic parameters [conformational free energy difference $\Delta G°$ and free energy of activation $\Delta G^{‡}$] of model compounds **1**−**4** in solution and of **1**, **5**, and **6** in the solid state (from X-ray crystal measurements) (Scheme 1). A detailed computational study for the open-chain hydrazone forms found for most of the compounds will be reported in a separate paper.

Results and Discussion

Compounds 1−3. In the solid state, **1** adopts a cycloheptadiene-like boat conformation (**B**, Figure 1), where six atoms (C-5a, C-5, N-4, N-3, the carbonyl oxygen, and the (N-4)-methyl carbon) are almost coplanar, with an interplanar angle of ca. 30° to the plane of the benzofusion, as shown by X-ray diffraction. The amide C−N bond length is 1.335 Å, intermediate between the single-bond length of 1.47 Å and the double-bond length of 1.24 Å.[10] The N-1−C-9a bond is shorter than the N-1−C-2 bond and comparable with the amide C−N bond length in this molecule as well as in the open-chain structures of the model compounds **5** and **6** (see below). Summation of the three valence angles around N-4, N-1, and N-3 gave 357.8°, 347.3°, and 337.6°, respectively, indicating the close sp^2 character of the first two atoms.

Table 1. Comparison of X-ray Crystallographic and PM3-Calculated Parameters of 1

	X-ray	PM3
Bond Lengths (Å)		
N-1−C-2	1.484(5)	1.499
C-2−N-3	1.437(5)	1.501
N-3−N-4	1.405(5)	1.436
N-4−C-5	1.355(5)	1.418
C-5−O1	1.233(6)	1.224
C-5−C-5a	1.486(7)	1.489
C-5a−C-6	1.390(6)	1.403
C-6−C-7	1.384(7)	1.384
C-7−C-8	1.369(8)	1.394
C-8−C-9	1.378(7)	1.382
C-9−C-9a	1.400(6)	1.414
C5a−C9a	1.394(6)	1.408
C-2−C(Me)	1.525(8)	1.535
N-4−C(Me)	1.453(7)	1.481
N-1−H	0.80(5)	0.997
Bond Angles (deg)		
N-1−C-2−N-3	110.7(4)	113.1
C-2−N-3−N-4	114.6(4)	115.0
N-3−N-4−C-5	122.3(4)	121.5
N-4−C-5−C5a	118.0(4)	120.7
C-2−N-1−C9a	120.2(3)	128.2
Dihedral Angles (deg)		
N-1−C-2−N-3−N-4	−47.5(5)	−65.8
C-2−N-3−N-4−C5	80.7(5)	72.8
N-3−N-4−C-5−C5a	−13.5(6)	−5.6
N-3−C-2−N-1−C-9a	−38.5(6)	0.0
C-5a−C-5−N-4−C(Me)	−176.1(4)	−179.0
C-6−C5a−C-5−O	−31.5(6)	−36.8
C-9a−N-1−C-2−C(Me)	79.9(6)	117.2
C-9a−N-1−C-2−C(Me)	−159.7(5)	−125.0

The assumption that the low-temperature conformer of **1** in solution[6a] is the same as that found in the crystals prompted us to investigate this molecule by the MM and semiempirical techniques mentioned above. The MMX minimization of **1** under a complete release of all constraints gave a structure which was transferred to the MOPAC software for AM1, PM3, and MNDO MO calculations. A similar boat (**B**) conformer was found to reproduce the crystal structure of **1** (see Figures 1a and 1b). A geometrical and conformational comparison of some crystallographic and PM3-calculated parameters is shown in Table 1. The calculated values are in good agreement with the X-ray results. The parameters relating to the amide moiety of the seven-membered ring seem to agree better than those for the rest of the ring.

It has been noted that the different modes of conformational interconversion associated with the lowest barriers between minimum energy conformers display fascinating patterns of well-coordinated atomic movement.[11] An inspection of Dreiding models of both **1** and **4** shows that, due to the constraints imposed by the amide moiety, there can be four probable pathways of ring interconversion, discussed earlier by others[1a] (see Figure 2; the case of **4** is demonstrated). The pseudorotation process involves the transformation of boat **B**

(6) (a) For Part 1 see Pihlaja, K.; Simeonov, M. F.; Fülöp, F. *J. Org. Chem.* **1997**, *62*, 5080. (b) Allinger, N. L. *J. Am. Chem. Soc.* **1977**, *99*, 8127.
(7) Dewar, M. J. S.; Thiel, W. *J. Am. Chem. Soc.* **1977**, *99*, 4899.
(8) Dewar, M. J. S.; Zoebisch, E. G.; Healy, E. F.; Stewart, J. J. P. *J. Am. Chem. Soc.* **1985**, *107*, 3902.
(9) Stewart, J. J. P. *J. Comput. Chem.* **1989**, *10*, 209, 221.
(10) Robin, M. B.; Bovey, F. A.; Basch, H. *The Chemistry of Amides*; Zabinsky, J., Ed.; Interscience Publishers: London, 1970.
(11) Kolossvary, I.; Guida, W. C. *J. Am. Chem. Soc.* **1993**, *115*, 2107.

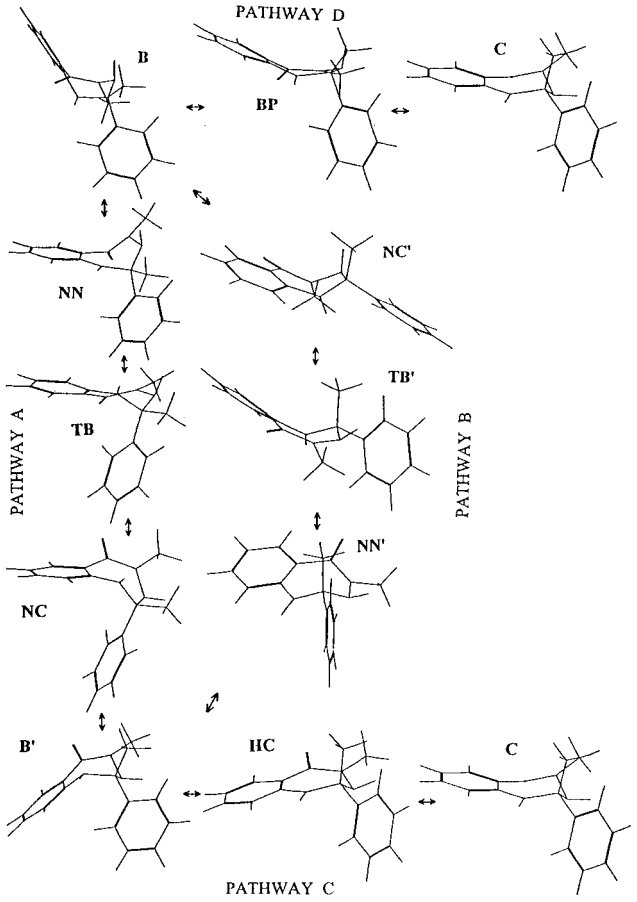

Figure 2. Computer-generated projections of the PM3-calculated conformations of **4** for ring transformations following the pathways A−D.

to inverted boat **B′** via twist-boat **TB** and 1,2-biplanar (**NN** and **NC**) forms via two different routes: (A) the wagging of C-2 (**B↔NN↔TB↔NC↔B′**); and (B) the wagging of N-4 (**B↔NC′↔TB′↔NN′↔B′**). Additionally, the **C↔B′** and the **C↔B** ring rotations involve two different mechanisms: (C) the wagging of the phenyl C═C bond through the **HC** or envelope state to the **B′** form; and (D) the wagging of N-3 through a biplanar transition state (**BP**, with five ring atoms essentially coplanar) to boat **B**. Starting from the optimized boat form of **1**, an extensive modeling of all transition states was generated with the aid of the ring-dihedral driver option of the PCMODEL[12] (see the Experimental Section). These geometry parameter files for structures of interest were then transferred to the MOPAC software package. The calculated heats of formation $\Delta H_f°$ (MMX ΔE values in the case of MM calculations) and relative energies $\Delta\Delta H_f°$ of **1** are given in Table 2 and the projectives in Figure 2 (the case of **4** is shown; see below).

The calculations result in **B** forms with very close energies: within 1−2 kcal mol^{-1} from MMX and PM3, and within *ca*. 4 kcal mol^{-1} from AM1 and MNDO. The experimental conformational energy difference $\Delta G°_{\mathbf{B}\leftrightarrow\mathbf{B}'}$ 2.5 kcal mol^{-1} (only one ring form was observed) agrees well with the AM1 and MNDO and even MMX and PM3 calculations. The other low-energy form is the chair **C**, whose energy relative to the boat **B** drastically decreases from 24.3 kcal mol^{-1} (MMX) to *ca*. 3 kcal mol^{-1} (PM3 and MNDO), and by MNDO calculations it is even *ca*. 1 kcal mol^{-1} below that of the **B′** form. Additionally, MMX and AM1 locate a **TB** form at a minimum in the pseudorotation circuit (A). As to the energy profile of the probable pathways A−D, all methods give the same qualitative picture: the lowest energy process is the **B↔B′** pseudorotation via the wagging of C-2 (A); energetically slightly higher are the ring flippings from **B′** to **C** form through an **HC** transition state (pathway C), and from a **B** to a **B′** form through pathway B, whereas that via pathway D is much higher. These results (Table 3) reproduce quite well the experimental finding that the highest mobility of the ring relates to the moiety including C-2 and N-4. Also, MNDO gives reliable values for the energy barrier of pathway A. Thus, as a whole AM1 reproduces the conformational energy barrier best. If only the most probable pathway of interconversion (A) is considered, both AM1 and MNDO give satisfactory agreement with the experimental results. The (N-3)-H

(12) Program PCMODEL/MMX, Serena Software, Bloomington, IN.

Table 2. Calculated Heats of Formation[a] $\Delta H_f°$ (kcal mol^{-1}) and Relative Heats of Formation $\Delta\Delta H_f°$ (in parentheses) of Compound 1

form[b]	MMX	AM1	PM3	MNDO
B	9.1 (0.0)	36.2 (0.0)	12.7 (0.0)	24.9 (0.0)
HC	34.1 (25.0)	47.5 (11.3)	21.2 (9.5)	41.2 (16.3)
C	33.3 (24.2)	43.7 (7.5)	16.1 (3.4)	28.1 (3.2)
BP	73.8 (64.7)	75.4 (39.2)	46.0 (33.3)	61.5 (36.6)
B′	10.2 (1.1)	40.3 (4.1)	14.3 (1.6)	29.2 (4.3)
NN	22.3 (13.2)	41.7 (5.5)	15.1 (2.4)	30.5 (5.6)
TB	17.2 (8.1)	41.2 (5.0)	16.7 (4.0)	33.2 (8.3)
NC	28.5 (19.4)	45.8 (9.6)	18.5 (5.8)	36.7 (11.8)
NC′	39.9 (30.8)	43.3 (7.1)	16.4 (3.7)	29.4 (4.5)
TB′	28.3 (19.2)	48.2 (12.0)	21.5 (8.8)	40.8 (15.9)
NN′	17.7 (8.6)	45.3 (9.1)	18.6 (5.9)	37.6 (12.7)
N3	34.9 (25.8)	47.3 (11.1)	20.7 (8.0)	34.0 (9.1)

[a] MMX energies in MM calculations. [b] See the projectives in Figures 2 and 3.

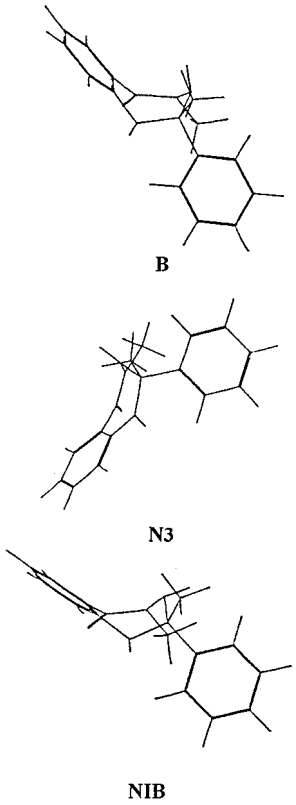

Figure 3. Computer-generated projections of the PM3-calculated conformations of **4** for N-3 nitrogen inversion process.

Table 3. Energy [$\Delta H_f°$ and $\Delta\Delta H_f°$ (see Table 2), kcal mol^{-1}] Profile Calculated for Interconversion Pathways of Compound 1

	pseudorotation				ring rotation				
	pathway A: **B↔B′** (wagging of C-2) (via **TB** form)		pathway B: **B↔B′** (wagging of N-4) (via **TB′** form)		pathway C: **B′↔C** (wagging C=C) (via **HC** form)		pathway D: **B↔C** (wagging N-3) (via **BP** form)		N-3$_{inv}$ (via **N3** form)
	$\Delta H^{‡}$ [a]	$\Delta\Delta H_f°$	$\Delta H^{‡}$ [b]	$\Delta\Delta H_f°$	$\Delta H^{‡}$ [c]	$\Delta\Delta H_f°$	$\Delta H^{‡}$ [d]	$\Delta\Delta H_f°$	$\Delta H^{‡}$ [e]
MMX	19.4	1.1	30.8	1.1	23.9	23.2	64.8	24.2	25.8
AM1	9.6	4.1	12.0	4.1	7.2	3.4	39.2	7.5	11.1
PM3	5.8	1.6	8.8	1.6	6.9	1.8	33.3	3.4	8.0
MNDO	11.8	4.3	15.9	4.3	12.0	−1.1	36.6	3.2	9.1
EXP.	13.0	>2.5							<13.0

[a] Calculated from $\Delta H_f°_{(NC)} - \Delta H_f°_{(B)}$ and considered as energy barrier (*cf.* Table 2). [b] Calculated from $\Delta H_f°_{(TB')} - \Delta H_f°_{(B)}$ (*cf.* Table 2). [c] Calculated from $\Delta H_f°_{(HC)} - \Delta H_f°_{(B')}$ (*cf.* Table 2). [d] Calculated from $\Delta H_f°_{(BP)} - \Delta H_f°_{(B)}$ (*cf.* Table 2). [e] Calculated from $\Delta H_f°_{(N3)} - \Delta H_f°_{(B)}$ (*cf.* Table 2).

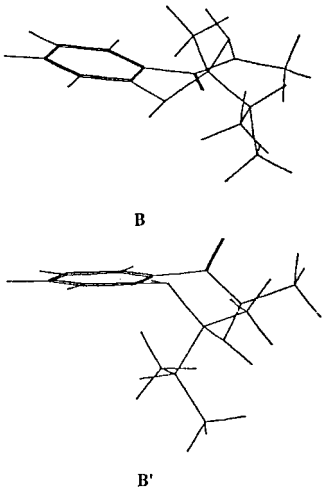

Figure 4. Computer-generated projections of the PM3-calculated boat (**B**) and inverted boat (**B′**) conformations of compound **2**.

Table 4. Stability Differences ($\Delta\Delta H_f°$, kcal mol^{-1})[a] between Boat (B) and Inverted Boat (B′) Forms for Compounds 1−4

	1	**2**	**3**	**4**
MMX	1.1	0.4	−1.4	2.5
AM1	4.1	1.3	0.6	1.9
PM3	1.6	−1.6	−2.7	0.1
MNDO	4.3	0.0	0.0	0.6

[a] The negative sign means a lower energy for the **B′** form.

nitrogen inversion process (Figure 3; the case of **4** is demonstrated) also seems to be well reproduced by the semiempirical calculations: AM1, MNDO, and PM3 gave energy barriers of *ca.* 11, 9 and 8 kcal mol^{-1}, respectively, as compared with the experimental value of less than 13 kcal mol^{-1}. These values represent the transition state (**N3**) with the (N-3)-H proton in the plane formed by C-2, N-3, and N-4. Thus, both the theoretically calculated energies and the NMR parameters fit well to a rapid **B** to **B′** pseudorotation flipping, which can be attributed to the not too different steric requirements in the two boat forms of **1**.

The calculated differences between the heats of formation ($\Delta H_f°$) of the **B** and **B′** forms of **1**−**4** (projectives for **2** in Figure 4) are given in Table 4. The experimental results discussed above permit the suggestion that (i) the **B′** conformation is favored for **2** and **3**, with the bulky isopropyl and *tert*-butyl groups at C-2 locating "away" from the (N-4)-methyl group, and (ii) the qualitative observations of the steric effect of the bulky alkyl groups

Table 5. Calculated Heats of Formation[a] $\Delta H_f°$ (kcal mol^{-1}) and Relative Heats of Formation $\Delta\Delta H_f°$ (in parentheses) of Compound 4

form[b]	MMX	AM1	PM3	MNDO
B	19.8 (0.0)	70.1 (0.0)	42.3 (0.0)	60.8 (0.0)
HC	47.8 (28.0)	83.2 (13.1)	57.5 (15.2)	78.2 (17.4)
C	45.3 (25.5)	72.0 (1.9)	44.6 (2.3)	62.9 (2.1)
BP	63.1 (43.3)	95.4 (25.3)	70.7 (28.4)	87.4 (26.6)
B′	22.3 (2.5)	72.0 (1.9)	42.4 (0.1)	61.4 (0.6)
NN	32.6 (12.8)	79.9 (9.8)	52.3 (10.0)	65.7 (4.9)
TB	28.2 (8.4)	79.3 (9.2)	54.2 (11.9)	69.2 (8.4)
NC	50.4 (30.6)	84.4 (14.3)	56.8 (14.5)	76.0 (15.2)
NC′	52.0 (32.2)	81.0 (10.9)	54.4 (12.1)	70.0 (9.2)
TB′	42.6 (22.8)	85.2 (15.1)	58.6 (16.3)	79.0 (18.2)
NN′	30.1 (10.3)	81.6 (11.5)	55.2 (12.9)	76.4 (15.6)
N3	42.3 (22.5)	83.3 (13.2)	57.4 (15.1)	71.3 (10.5)

[a] MMX energies in MM calculations. [b] See the projectives in Figures 2 and 3.

are reproduced better by the PM3 than by the AM1 and MNDO calculations. The $\Delta H_f°$ values calculated with PM3 for **2** and **3** range from slightly above to slightly below 2 kcal mol^{-1}, in favor of the **B′** form, whereas AM1 prefers the **B** form and the MNDO calculations show no preference.

Compound 4. An inspection of Dreiding models shows that the upfield shifts of the (C-2)-methyl protons from 1.79 and 1.62 ppm at 273 K to 1.66 and 1.50 ppm at 192 K and of the (N-4)-methyl protons from 2.66 to 2.51 ppm, and the downfield shifts of the N-1 and N-3 protons to 5.3 and 4.7 ppm, respectively,[6a] can be explained by the proposed changes in ring conformations where the phenyl ring rotation around the C-2−C-1′ bond can affect the above chemical shifts via the ring current factors.

The calculated heats of formation $\Delta H_f°$ (MMX ΔE values in the case of MM calculations) and the relative energies $\Delta\Delta H_f°$ of **4** are given in Table 5. The PM3-calculated ring torsional angles for all conformations are given in Table 6 and their projectives in Figures 2 and 3. The calculations result again in the **B** forms having lowest energy. The conformational energy difference between the two boat forms was found from PM3 and MNDO approximations to be less than 1 kcal mol^{-1}, in good agreement with the experimental observations. The energy profile of the probable pathways A−D (Table 7) extracted from our molecular modeling of **4**, as in the case of **1**, shows that all methods give the same qualitative picture: the lowest energy process is that of **B↔B′** pseudorotation via the wagging of C-2 (A), the energetically higher is the ring flipping from a **B′** to a **C** form via the wagging of the C=C bond through an **HC** state (route

Table 6. PM3-Calculated Ring Torsional Angles for Conformational Forms of 4

angle (deg)	B	HC	C	BP	B′	NN	TB	NC	NC′	TB′	NN′	FLAT
N-1−C-2−N-3−N-4	−69.2	64.2	74.8	−7.3	48.4	−58.2	−62.0	2.6	1.0	34.1	62.3	1.5
C-2−N-3−N-4−C-5	76.5	−53.6	−77.9	16.8	−60.8	−10.2	1.2	−55.1	68.0	14.9	−0.7	13.8
N-3−N-4−C-5−C5a	−5.0	5.3	76.1	15.2	−16.0	72.5	39.5	24.1	−61.4	−14.8	−43.7	−10.0
N-4−C-5−C-5a−C-9a	−39.6	19.2	−52.1	−37.1	57.1	−48.6	−13.3	34.3	−0.4	−23.6	19.9	−4.9
N-1−C-9a−C-5a−C-5	8.0	−6.1	−4.2	6.7	1.4	−3.5	−13.0	−17.0	9.7	18.3	8.4	5.7
C-2−N-1−C-9a−C-5a	31.3	4.6	60.6	34.0	−70.2	−3.7	−21.1	−53.3	41.5	41.9	23.0	11.0
N-3−C-2−N-1−C-9a	1.1	−5.3	−78.2	−30.9	37.1	57.2	72.4	66.4	−60.0	−73.2	−73.2	−16.7
C-6−C-5a−C-5−O	−37.7	20.3	−44.9	−38.7	49.4	−42.4		29.4	−2.4	−20.1	17.4	−1.1
C-9−C-9a−N-1−H	20.0	−2.1	1.9	18.5	−11.2	0.9		−28.1	22.4	26.4	11.0	6.5

Table 7. Energy [$\Delta H_f°$ and $\Delta\Delta H_f°$ (see Table 5), kcal mol^{-1}) Profile Calculated for Interconversion Pathways of Compound 4

	pseudorotation				ring rotation				
	pathway A: **B↔B′** (wagging of C-2) (via **TB** form)		pathway B: **B↔B′** (wagging of N-4) (via **TB′** form)		pathway C: **B′↔C** (wagging C=C) (via **HC** form)		pathway D: **B↔C** (wagging N-3) (via **BP** form)		N-3$_{inv}$ (via **N3** form)
	$\Delta H^{\ddagger}$ [a]	$\Delta\Delta H_f°$	$\Delta H^{\ddagger}$ [b]	$\Delta\Delta H_f°$	$\Delta H^{\ddagger}$ [c]	$\Delta\Delta H_f°$	$\Delta H^{\ddagger}$ [d]	$\Delta\Delta H_f°$	$\Delta H^{\ddagger}$ [e]
MMX	30.6	2.5	22.8	2.5	25.5	23.0	43.3	25.5	22.5
AM1	14.3	1.9	15.1	1.9	11.2	0.0	25.3	1.9	13.2
PM3	14.5	0.1	16.3	0.1	15.1	2.2	28.4	2.3	15.1
MNDO	15.2	0.6	18.2	0.6	16.8	1.5	26.6	2.1	10.5
EXP.	14.7	0.3							*ca.* 15

[a] Calculated from $\Delta H_f°_{(NC)} - \Delta H_f°_{(B)}$ and considered as energy barrier (*cf.* Table 5). [b] Calculated from $\Delta H_f°_{(TB')} - \Delta H_f°_{(B)}$ (*cf.* Table 5). [c] Calculated from $\Delta H_f°_{(HC)} - \Delta H_f°_{(B)}$ (*cf.* Table 5). [d] Calculated from $\Delta H_f°_{(BP)} - \Delta H_f°_{(B)}$ (*cf.* Table 5). [e] Calculated from $\Delta H_f°_{(N3)} - \Delta H_f°_{(B)}$ (*cf.* Table 5).

Table 8. Differences ($\Delta\Delta H_f°$, kcal mol^{-1})[a] between Enthalpies of Formation for the Boat (B) and N-3 Inverted Boat (NIB) Forms and for Those of the Inverted Boat (B′) and N-3 Inverted Boat (NIB′) Forms for Compounds 1−4

	1	2		3		4	
	NIB	NIB	NIB′	NIB	NIB′	NIB	NIB′
MMX	1.1	1.1	−1.6	1.2	−1.3	1.0	−1.3
AM1	3.3	2.5	−3.2	2.1	−3.7	2.0	−0.8
PM3	−0.3	−0.8	0.7	−2.6	−1.4	0.2	−1.0
MNDO	1.6	0.8	−2.7	1.2	−1.9	−0.1	−1.4
EXP.						0.3	

[a] The negative sign means a lower energy for the **NIB** or **NIB′** forms.

C) and then pathways B and D. The energy barriers calculated for pathways A−C with PM3, AM1, and MNDO are within 11−18 kcal mol^{-1}, and the PM3 values (*ca.* 15 kcal mol^{-1}), in contrast to the case of **1**, are in best agreement with the experimental findings.

Taking into account the results for **1**−**3** (Table 4) discussed above, our conclusion is that the PM3-calculated $\Delta\Delta H_f°_{(B↔B')}$ values reproduce quite satisfactorily all our experimental findings. Thus, both experimental and theoretical results show that in the compounds studied a phenyl substituent at C-2 has lower steric requirements than a methyl group.

As concerns the third experimentally observed form in **4**,[6a] we can speculate that this is a result of the *N*-3 inversion process now going on in the **B** forms with an energy of activation of *ca.* 15 kcal mol^{-1}, a value higher than that observed in **1** (*ca.* 13 kcal mol^{-1}, see above) and this simultaneously with the ring flipping process. The results of PM3 and AM1 calculations for the intermediate pathway of the nitrogen inversion (as generally assumed via a transition state corresponding to coplanar nitrogen,[13] see Figure 3) are in close agreement with the experimental data, giving values of 15.2 and 13.2 kcal mol^{-1}, respectively, but the MNDO method underestimates the inversional potentials for **4**, as for **1**.

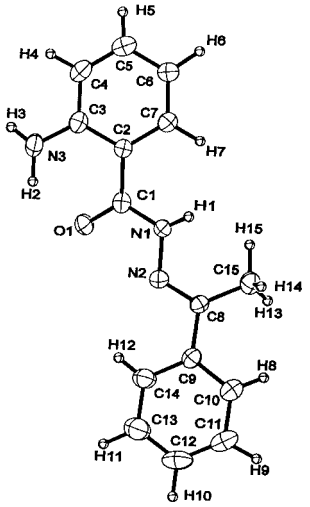

5

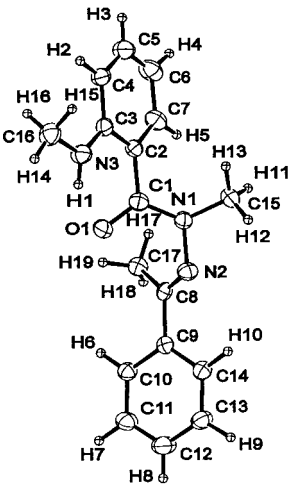

6

Figure 5. Structures in the crystals (ORTEP drawings) of compounds **5** and **6**.

Moreover, our calculations of the $\Delta H_f°$ of *N*-3 inverted conformers for the **B** and **B′** forms (**NIB** and **NIB′**, Table 8) reveal lower energy (*ca.* 1 kcal mol^{-1}) for the **NIB′** form of **4**. The PM3-calculated projectives of these forms are given in Figure 3. Hence, it seems that the PM3 calculations reflect quite well both the conformational energy differences and the energy barriers for **4**.

Open-Chain Forms (Hydrazones). To obtain an insight into the structures of our hydrazones in solution, X-ray analyses were carried out for model compounds **5** and **6**. The crystal structures of these compounds are shown in Figure 5. While **5** represents an almost completely flat molecule with a *trans*-amide bond (C=O anti to N−H) and azomethine *E*-configuration, **6** (closely

(13) Jennings, W. B.; Worley, S. D. *J. Chem. Soc., Perkin Trans. 2* **1980**, 1512.

Scheme 2

5 6

related to **4**) adopts a crystal structure with a torsion angle of 71.5° around N-3−N-4 (37.8° in **5**). Rotation around the N−N bond, which leads to the conformation where the lone pair of the tricoordinate nitrogen atom is orthogonal to the C=N π system (maximum energy), has already been encountered by others[14] in some *N*,*N*-diphenylhydrazones. We consider this phenomenon, which is much stronger in **6** than in **5**, to be a direct consequence of N-methylation in the former, leading to an energetically "compromised" structure with the N-4 methyl group on the opposite side to the (C-2)-methyl group and in a nearly orthogonal position to the carbonyl group to avoid severe steric hindrance at the expense of the electronic requirements (Scheme 2).

In order to investigate the *cis*/*trans* and *Z*/*E* preferences, and also the phenomenon of N−N rotation as a function of structure, MM and semiempirical MO calculations are in progress for these and other model compounds.

Experimental Section

Computations. Each structure was first solved by using PCMODEL Ver 4.25[12] program running at 33 MHz on an AT 486DX computer. The program uses the MMX[12] force-field method based on MM2 and MMPI p-subroutine programs developed by Allinger.[6b] The program was run throughout this study because of its speed of operation and the convenience of graphical input and output.[15] The D-DRIVER option was used for energy computation versus torsional rotation about the ring bonds. The ring atoms (with the exception of C-2 and N-3) were designated "π-atoms", which direct the program to utilize an iterative variable-electronegativity−self-consistent field (VESCF) procedure to reduce bond stretch force constants and twofold symmetry V2 torsional parameters associated with these atoms from their preassigned "double bond" values according to a scaling function based on VESCF-calculated bond order.[16] From the optimized geometries, input files were generated for the MOPAC Ver 6.12[17] calculations and for the ALCHEMY III[18] program to produce the projections of Figures 1b and 2−4. The same input files were run under the default MNDO, AM1, and the PM3 Hamiltonian, which was augmented and improved for heteroatom (N, O, *etc*.) calculations. In all cases the Eigenvector Following (EF) procedure gave full geometry optimization, and the PRECISE option was implemented as recommended[19] for augmenting the SCF convergence and geometry optimization criteria.

X-ray Structure Determinations.[22] Single crystal data collections were performed at 295 K with Rigaku AFC5S diffractometer using monochromatized Mo-K_α radiation (λ = 0.71096 Å).

For compound **1**, $C_{11}H_{15}N_3O$, a colorless prismatic crystal with dimensions 0.20 × 0.20 × 0.20 mm was used. The unit cell parameters were determined by least-squares refinements of 22 carefully centered reflections (10° < 2θ < 23°). The data obtained were corrected for Lorentz and polarization effects and for dispersion. A total of 1133 reflections were collected by ω−2θ scan mode ($2\theta_{max}$ = 50°), giving 1034 unique reflections (R_{int} = 0.029). Of those, 668 were considered as observed according to the criterion $I > 3\sigma(I)$. The three check reflections monitored after every 150 reflections showed only statistical fluctuations during the course of the data collection.

Table 9. Summary of Crystal Data, Intensity Collection, and Structure Refinement Parameters for Compounds 1, 5, and 6

compound	**1**	**5**	**6**
formula	$C_{11}H_{15}N_3O$	$C_{15}H_{15}N_3O$	$C_{17}H_{19}N_3O$
M_r	205.26	253.30	281.36
crystal system	monoclinic	orthorhombic	triclinic
space group	$P2_1$ (No. 4)	$Pna2_1$ (No. 33)	P1 (No. 2)
a, (Å)	7.713(3)	8.594(5)	8.324(2)
b, (Å)	8.550(2)	5.784(4)	12.400(2)
c, (Å)	9.035(2)	26.520(6)	7.865(2)
α, deg	90	90	94.66(2)
β, deg	111.49(3)	90	105.28(2)
γ, deg	90	90	93.44(2)
V, Å^3	554.4(6)	1318(2)	777.7(6)
Z	2	4	2
D_c, g cm^{-3}	1.229	1.276	1.201
μ (Mo K$_\alpha$), cm^{-1}	0.77	0.77	0.72
F(000)	220	536	300
measured reflections	1133	1410	2948
unique reflections	1054	1410	2742
obs reflections, $I > 3\sigma(I)$	668	790 (2σ)	1028
R^a	0.035	0.036	0.038
$R_w{}^b$	0.037	0.037	0.039
S^c	1.24	1.21	1.25

[a] $R = \sum(|F_o| - |F_c|)/\sum|F_o|$. [b] $R_w = [\sum w(|F_o| - |F_c|)^2/\sum w|F_o|^2]^{1/2}$, with $w = 1/\sigma^2(F_o)$. [c] $S = [\sum w(|F_o| - |F_c|)^2/(m - p)]^{1/2}$.

The structure was solved by direct methods using MITRIL.[20] Least-squares refinements and all subsequent calculations were performed using the TEXSAN[21a] crystallographic software package, which minimized the function $\sum w(\Delta F)^2$ when $w = 1/\sigma^2(F_o)$. Refinement of all non-hydrogen atoms with anisotropic and hydrogen atoms with fixed isotropic temperature parameters (1.2 times B_{eq} of carrying atom) reduced the *R* value to 0.035 (R_w = 0.037) for 180 parameters. Neutral atom scattering factors were those included in the program. Structures were plotted with ORTEP.[21b]

The unit cell dimensions of **5** were determined by least-squares refinements of 25 carefully centered reflections (21° < 2θ < 36°) and from 24 reflections (24° < 2θ < 37°) for **6**. The structures of **5** and **6** were solved and refined in the same way as for **1**. For **6** an absorption correction was also applied and the data were used according the criteria $I > 2\sigma(I)$. The final factors were given in Table 9.

Conclusions

(i) Only the combined use of experimental (1D and 2D NMR techniques, and X-ray spectroscopy) and computational (AM1, PM3, and MNDO molecular orbitals and MMX molecular mechanics) techniques allowed an insight into the ground-state structures and into the probable interconversion pathways of the dynamic processes studied.

(14) Shvo, Y.; Nahlieli, A. *Tetrahedron Lett*. **1970**, 4273.
(15) Gajewski, J. J.; Gilbert, K.; McKelvie, J. *Advances in Molecular Modelling*; JAI Press: Greenwich, CT, 1990.
(16) Burkert, U.; Allinger, N. L. *Molecular Mechanics*, ACS Monograph 177, American Chemical Society: Washington, DC, 1982.
(17) Stewart, J. J. P. FJSRL TR-90-0004, 1990.
(18) Tripos Associates, Inc., 1992.
(19) Boyd, D. B.; Smith, D. W.; Stewart, J. J. P.; Wimmer, E. *J. Comput. Chem*. **1988**, *9*, 387.
(20) Gilmore, C. J. *J. Appl. Crystallogr*. **1982**, *17*, 42.
(21) (a) TEXSAN-TEXRAY: Single Crystal Structure Analysis Package, Version 5.0, Molecular Structure Corporation, The Woodlands, TX, 1989. (b) Johnson, C. K. *ORTEP-II*, *Report ORNL-5138*; Oak Ridge National Laboratory: Oak Ridge, TN, 1976.
(22) The authors have deposited atomic coordinates for **1**, **5**, and **6** with the Cambridge Crystallographic Data Centre. The coordinates can be obtained, on request, from the Director, Cambridge Crystallographic Data Centre, 12 Union Road, Cambridge, CB2 1EZ, UK.

(ii) Both MMX molecular mechanics and semiempirical PM3, AM1, and MNDO molecular orbital calculations showed a close qualitative picture of the energy profiles of the possible interconversion pathways for the studied 2,2-disubstituted-1,3,4-benzotriazepinones, but only the PM3 calculations gave a reasonable agreement with the experimental estimates for the $\Delta G°$ values in **1**−**4**.

(iii) In general, PM3, AM1, and MNDO calculations reproduced both energy barriers and conformational energy differences for the studied compounds quite satisfactorily.

Acknowledgment. M.F.S. acknowledges a Fellowship from the Turku University Foundation and in part from the Academy of Finland.

JO962323C